Supporting Information

for

Photoelectrochemical Water Oxidations by a MOF/Semiconductor Composite

Bradley Gibbons, Daniel R. Cairnie, Benjamin Thomas, Xiaozhou Yang, Stefan Ilic, and Amanda J. Morris*

Department of Chemistry, Virginia Polytechnic Institute and State University, Virginia 24060, USA

Contents	Page

WO_3 paste preparation for ultrafast transient absorption (ufTA) measurements

WO_3 paste was prepared following a protocol by Gratzel et al. with some slight modifications.[1] The amount of WO_3 nanoparticles (SkySpring Nanomaterials) was diluted by a factor of $1/8^{th}$ by weight. The WO_3 powder was ground up in a mortar and pestle with sequential additions of water and ethanol to form a thick paste. The paste was then diluted with ethanol, and stirred 1 min. The homogenous suspension was then further dispersed using a tip sonicator (Branson Digital Sonifer) with a work/rest interval of 2 seconds on/off thirty times at 30% amplitude. To the mixture, α-terpineol (Sigma Aldrich) was added and the stirring/sonication process was repeated. A 10% solution (wt%) of ethyl cellulose in ethanol was then added to the WO_3 mixture and the stirring/sonication process was repeated. The mixture was then ball-milled at 600 rpm overnight with zirconia balls and the resulting paste was concentrated via rotary evaporator.

WO_3 film preparation for ufTA measurements

WO_3 films were prepared by doctor blading portions of the WO_3 paste over clean glass microscope slides (Thermo Scientific). The doctor-bladed films were covered with a beaker and left to air-dry for 30 min. The films were then transferred to a 120 °C oven to dry further for 1 h and annealed in a 500 °C furnace in air for 2 h. After cooling, the films were then used in synthesis.

Ru-UiO-67 film preparation for ufTA measurements

The Ru-UiO-67 and Ru-UiO-67/WO_3 films were prepared according to a previously published procedure, with slight modifications.[2] To a 6 dram vial, $ZrCl_4$ (58.3 mg, 0.25 mmol), biphenyl dicarboxylic acid (50.9 mg, 0.21 mmol), and $[Ru(tpy)(dcbpy)Cl]PF_6$ (41.5 mg, 0.055 mmol) were added along with DMF (10 mL) and glacial acetic acid (1.5 mL). The contents were sonicated for 5 min and either two glass slides or two WO_3-coated slides were placed facing up in the vial, with one across and the other placed along the vial wall. The vial was then capped and placed in a 120 °C oven for 20 h. The vials were then cooled, and the films were washed with DMF and acetone. The backside of the glass slides was wiped with a Kimwipe soaked in dilute NaOH. The films were soaked in acetone over two days and then air-dried overnight. Finally, the dry films were transferred to an N_2 glovebox and stored there until needed.

Preparation of films for ufTA

The films were placed into a custom quartz optical cell (Quark glass) with a 2 mm pathlength and a 19/22 female joint. The optical cell was sealed with a 19/22 rubber septum and purged with Ar for 30-45 min to remove any residual air.

Methods

A Bruker D8 Advance X-ray diffractometer was used to measure the X-ray diffraction of each film sample. SEM images were collected on a LEO/Zeiss 1550 field-emission scanning electron microscope. UV-Vis spectroscopy was conducted with a Cary 5000 UV-Vis-NIR spectrometer in water. All electrochemical experiments were preformed using a BASi Epsilon potentiostat in 0.1 M $LiClO_4$ electrolyte adjusted to pH=6 prior to analysis with HCl. All experiments used a Ag/AgCl reference electrode and a Pt mesh counter electrode. After all analysis a standard was measured, $K_3Fe(CN)_6$ with a blank FTO working electrode and used to adjust all potentials to NHE ($E_{1/2}$ = 0.361 V vs. NHE). O_2 production was measured with a Clarke-type dissolved oxygen probe (Unisense OX-NP) and confirmed by gas chromatography (Agilent Technologies 7890A GC System using an Agilent J&W GC Columns Select Permanent Gases/CO2 Molsieve

5A/Porabond Q Tandem column (part number: CP7429). During GC experiments, the temperature was held at 25 °C for 5 min then ramped to °150 over 5 min with a total flow rate of 37 mL/min and a split ratio of 10:1.). Illumination for bulk electrolysis was provided by a Xe arc lamp at 1 sun intensity. X-ray photoelectron spectroscopy (XPS) spectra were collected on a PHI 5000 Vera Probe III spectrometer using an aluminum anode X-ray source with photon energy of 1486.6 eV. Samples were digested for ICP-MS in 10 mL of concentrated HNO_3 and diluted to a final concentration of 2% HNO_3 and 0.5% HCl (w/w%). Film thicknesses and height profiles were probed using atomic force spectroscopy (AFM). The AFM images were acquired with a Jupiter-XR (Oxford Instruments Asylum Research) operating in tapping mode with an AC160TS-R3 (Olympus) cantilever. Raw data files were processed and analyzed in Ergo AFM software.

Ultrafast transient absorption (ufTA) measurements

Ultrafast transient absorption measurements were performed with a HeliosFire spectrometer (Ultrafast Systems). The 320 nm pump source was obtained by passing a portion of the 800 nm light generated by a Coherent Astrella ultrafast laser system (1 kHz, 35 fs FWHM) through an optical parametric amplifier (Apollo, Ultrafast Systems). Residual 800 nm light was directed into a mechanical delay stage (EOS, Ultrafast Systems) where the outputted light was focused onto a sapphire window to generate a white light continuum probe beam. The pump source was chopped to 500 Hz, while the probe beam remained at 1 kHz, so that every other probe pulse had no pump present. The pump beam polarization was perpendicular to the probe beam polarization. The pump beam spot size was determined by placing a pinhole wheel (Thorlabs, PHWM16) at the focus of the beam and a powermeter (Thorlabs, PM100D) with a sensor (Thorlabs, S401C) on the other side of the wheel. The diameter of the pinhole was progressively decreased while recording the power. Plotting power versus diameter yielded a pseudo-gaussian curve with an $1/e^2$ of ~250 μm. At a repetition rate of 500 Hz with 50 μW pump power, and a spot size of 250 μm, the energy density per pulse was ~200 $\mu J/cm^2$. The sample cell was placed in a mount and rastered over a 2 mm × 2 mm area throughout the measurements. The presented spectra are the averages over 3 different film areas. The instrument response function (IRF) was determined from the cross-phase modulation of a blank glass microscope slide excited with 320 nm light. The data obtained from the ufTA measurements was processed with the SurfaceXplorer software provided by Ultrafast Systems. The worked-up data was plotted with an Origin software package.

References

1. Lin, S. *et al.* Electrochemical Water Oxidation by a Catalyst-Modified Metal-Organic Framework Thin Film. *ChemSusChem* **10**, 514–522 (2017).
2. Lin, S. *et al.* Photoelectrochemical Alcohol Oxidation by Mixed-Linker Metal-Organic Frameworks. *Faraday Discuss.* (2020) doi:10.1039/D0FD00021C.

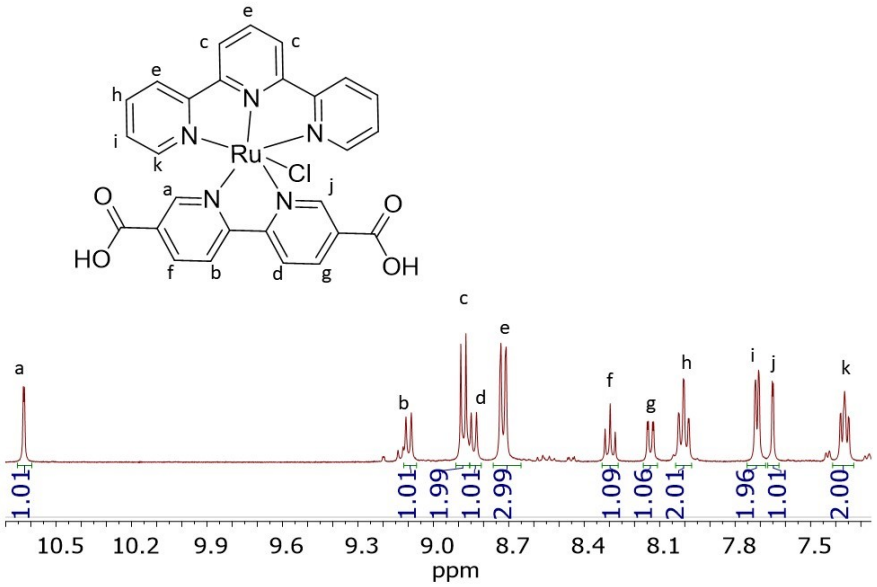

Figure S1. ^{1}H NMR of $[Ru(tpy)(dcbpy)Cl]PF_6$ in d_6-DMSO (400MHz).

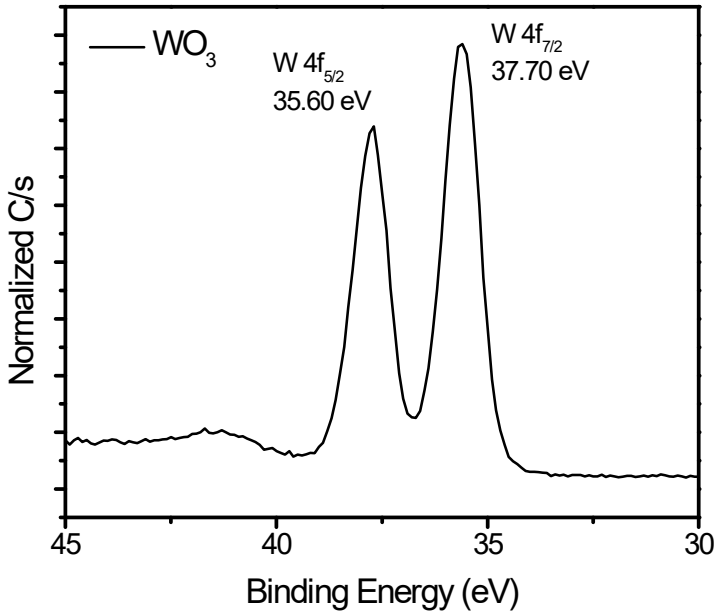

Figure S2. XPS of native WO_3 films prepared from a WCl_6 precursor solution.

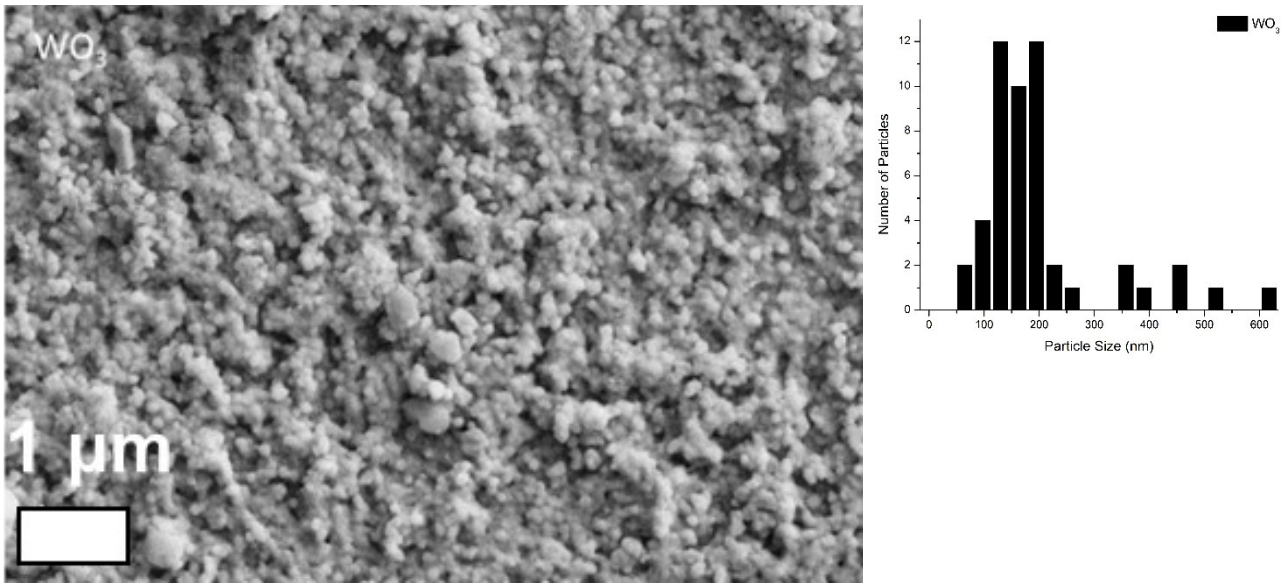

Figure S3. Scanning electron microscopy (SEM) image of a WO_3 film on FTO.

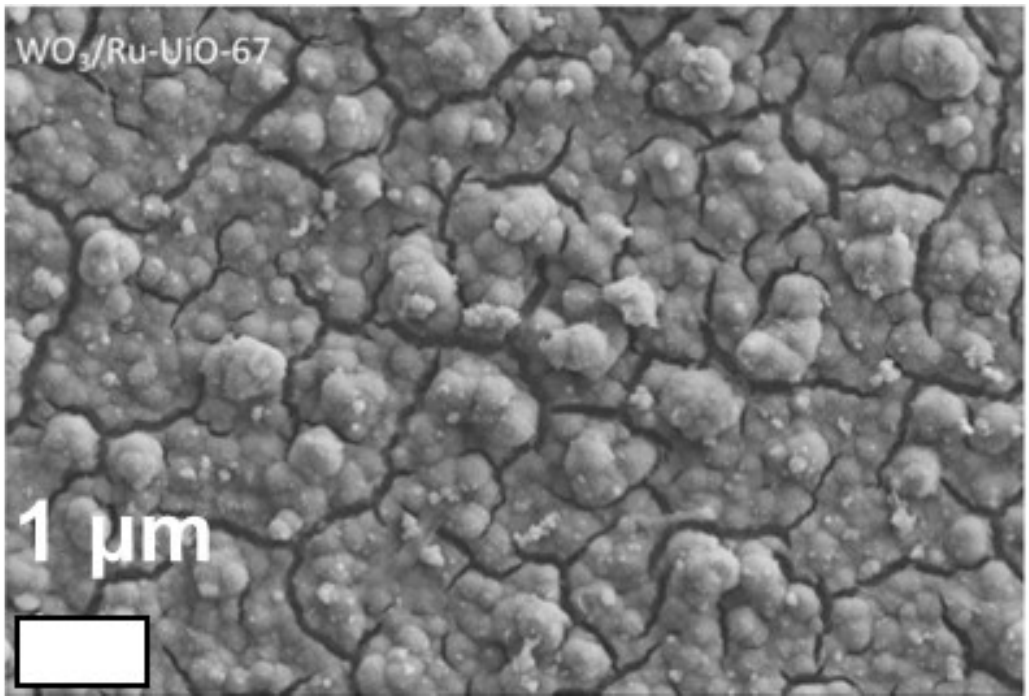

Figure S4. SEM image of a Ru-UiO-67/WO_3 film showing a uniform coverage of the WO_3 layer with the typical octahedral particle shapes that UiO-type MOFs exhibit.

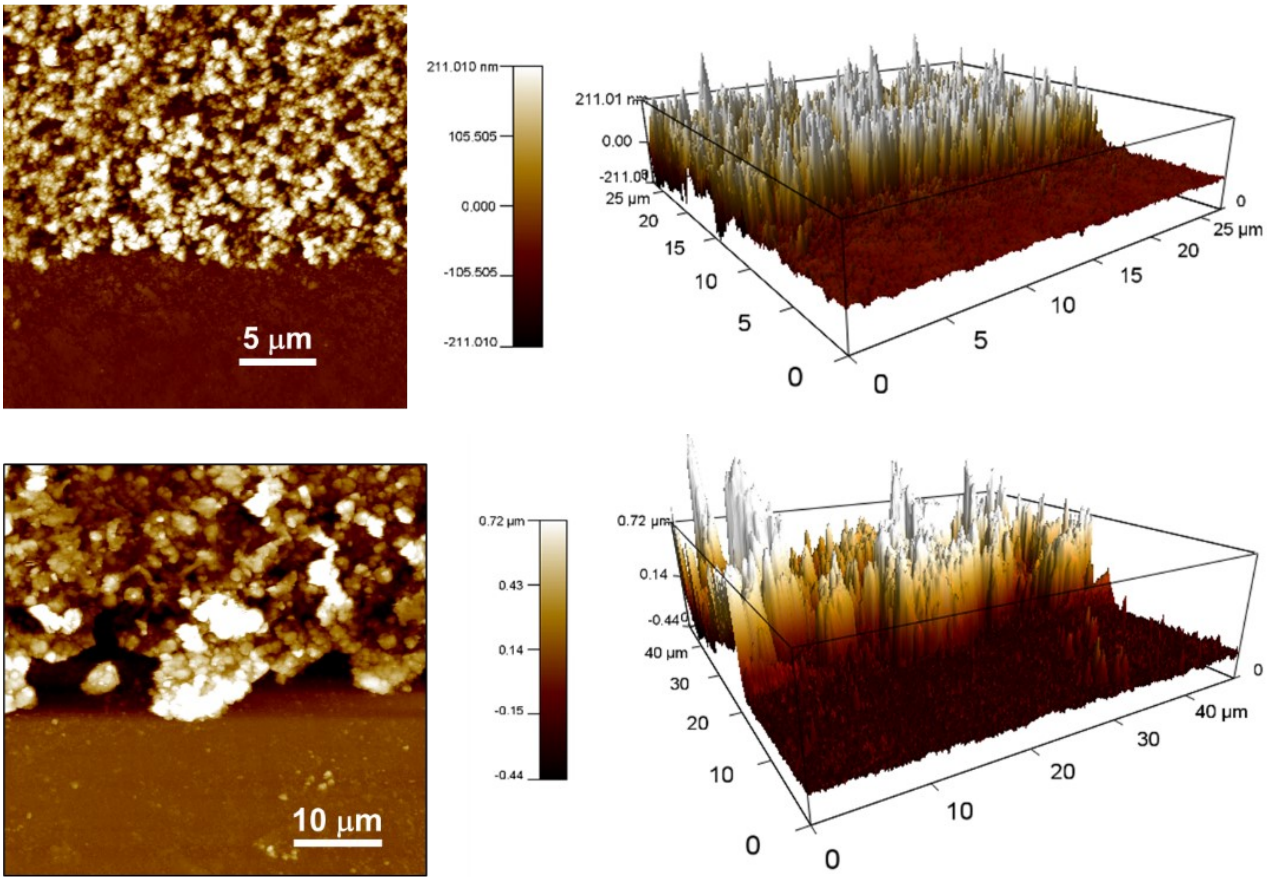

Figure S5. AFM profiles for WO_3 (top) and Ru-UiO-67/WO_3 (bottom) films.

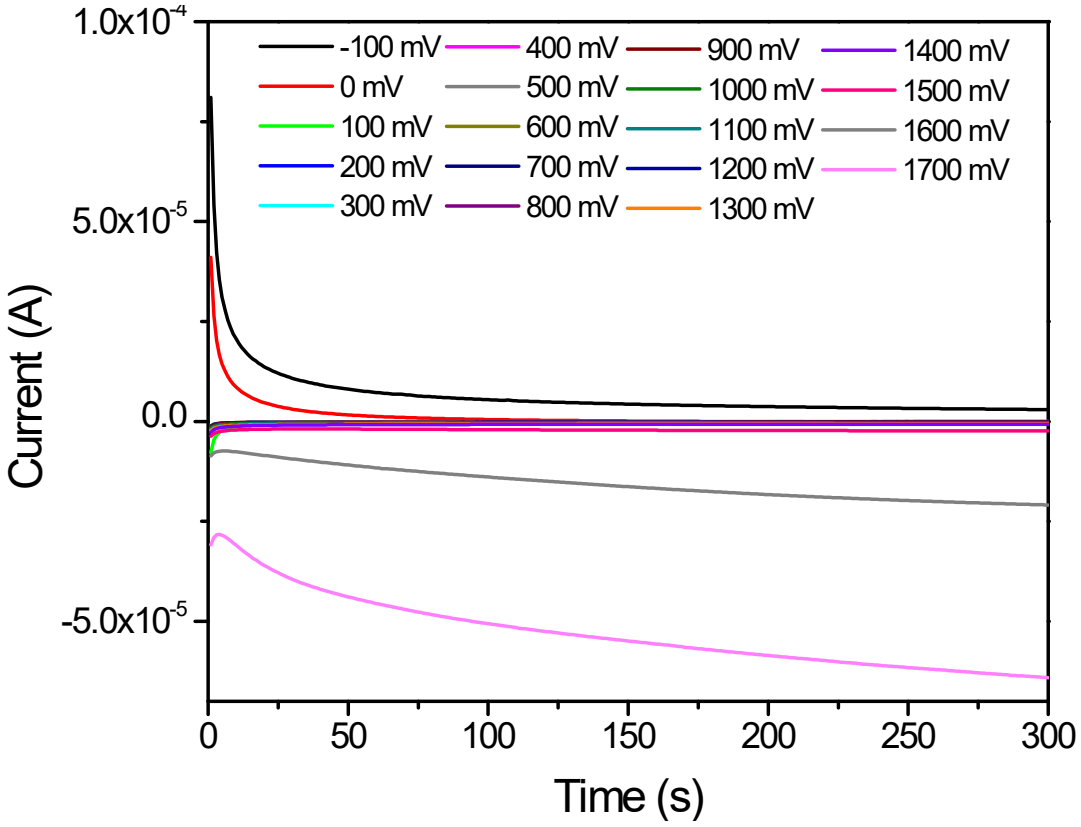

Figure S6. All chronoamperometry curves for steady state current measurements under dark conditions.

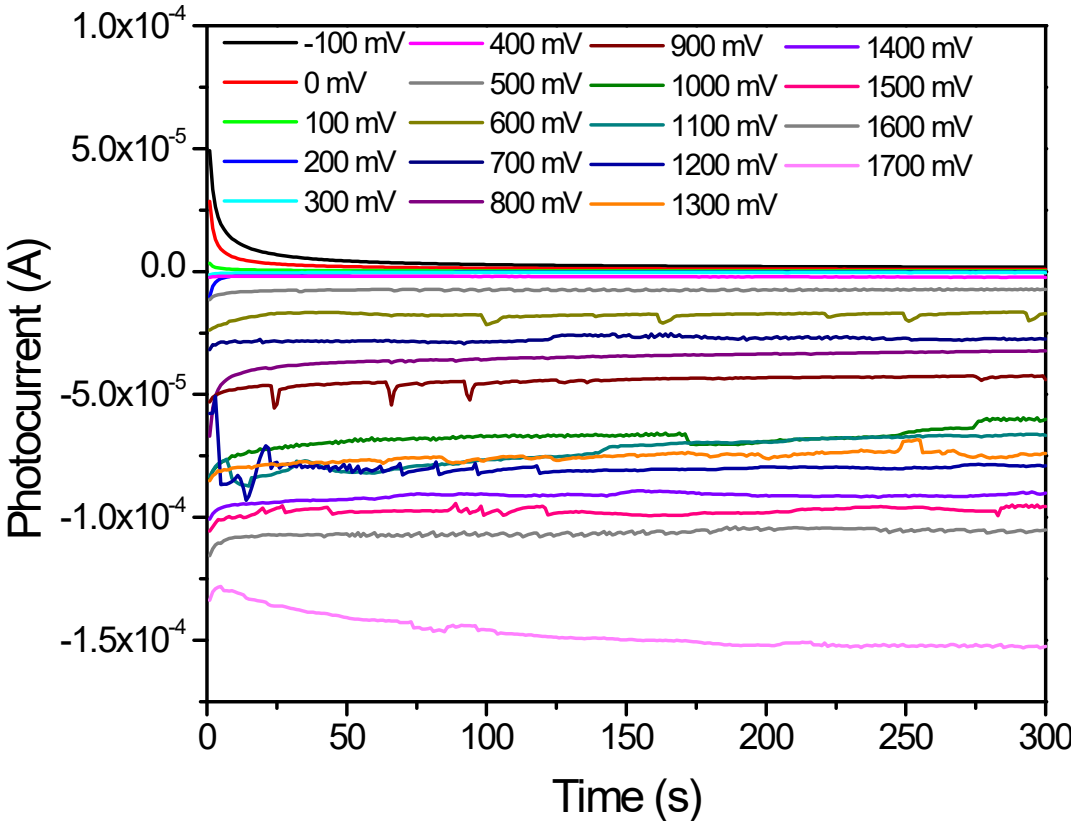

Figure S7. All chronoamperometry curves for steady state current measurements under light conditions.

Equations for Photo-response efficiency

The applied-bias photocurrent efficiency (ABPE) was determined with the following relation:

$$ABPE(\%) = \frac{J_{ph} \times (1.23\ eV - V)}{P_{total}} \#(1)$$

where J_{ph} is the photocurrent (mA/cm^2), V is the applied voltage (in volts), P_{total} is the power of the light source (in mW/cm^2), and 1.23 eV is the Gibbs free energy for the water oxidation reaction. The incident photon-to-current efficiency was determined with the equation below:

$$IPCE(\%) = \frac{J_{ph} \times 1239.8\ nm/eV}{P_{mono} \times \lambda} \#(2)$$

Where P_{mono} is the power of the light source at a given wavelength (mW), λ is the wavelength used (nm) and the constant 1239.8 nm/eV is a conversion factor from wavelength to eV. The equations needed to determine the efficiency of charge separation within the bulk electrode (η_{sep}) and charge transfer at the surface of the electrode to the electrolyte (η_{trans}) are:

$$\eta_{Trans} = \frac{J_{H_2O}}{J_{Na_2SO_3}} \#(3)$$

$$\eta_{sep} = \frac{J_{Na_2SO_3}}{J_{abs}} \#(4)$$

$$J_{abs} = \int_0^{\lambda} J_{Flux}(\lambda) d\lambda \#(5)$$

$$J_{Flux} = \frac{eN_a}{h\nu} \times LHE \#(6)$$

where J_{abs} is the integrated photocurrent (mA/cm^2) function of wavelength, J_{Flux} is the photocurrent at a given wavelength of irradiation (mW/cm^2), e is the charge of an electron (1.602 × 10^{-19} C), N_a is the photo flux ($photons \cdot s^{-1} \cdot cm^{-2}$) , $h\nu$ is the energy of a photon (Js) and LHE is calculated by:

$$LHE = 1 - 10^{-A(\lambda)} \#(7)$$

where $A(\lambda)$ is the absorbance of the film as a function of wavelength. J_{abs} was calculated for WO_3 and used for both films (2.49 mA/cm^2).

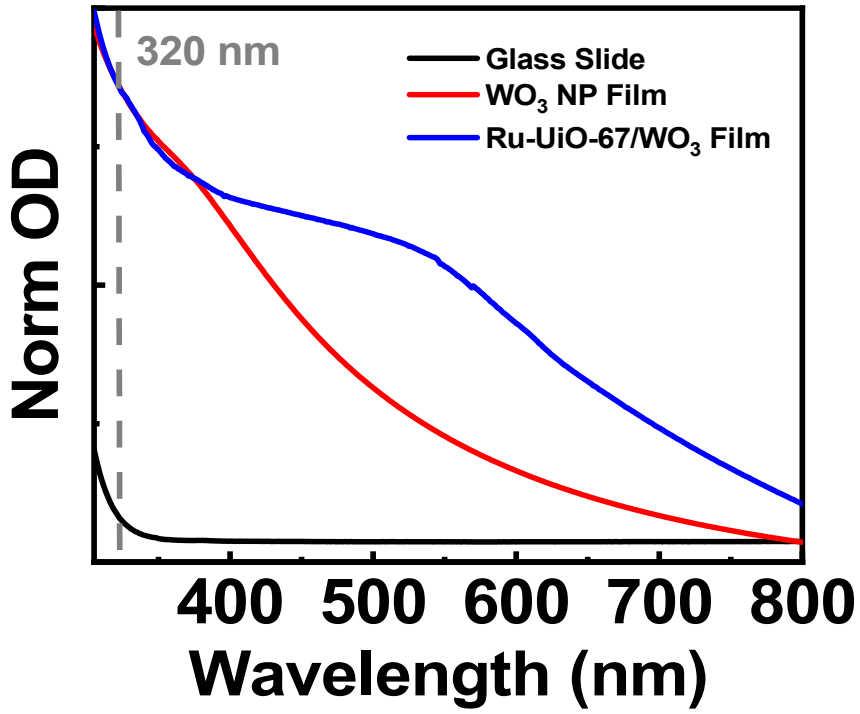

Figure S8. Absorption spectra of the glass slide, WO_3 and Ru-UiO-67/WO_3 thin films that were analyzed via ultrafast transient absorption measurements. For comparison, the non-normalized absorption spectra of the glass microscope slide where the films were grown on is provided (black line). The absorbance of the glass slide at the 320 nm excitation wavelength (grey dashed line) was 0.08, and any TA signal obtained with the glass slide (< 20 ΔμOD) was subtracted from the sample TA spectra prior to analysis.

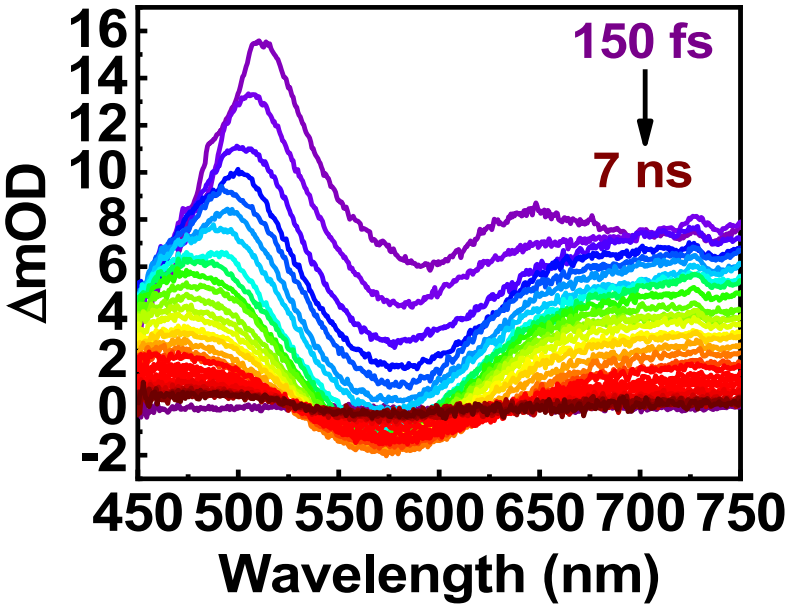

Figure S9. Ultrafast transient absorption spectral mapping (purple to red) of the Ru-UiO-67 film under an Ar atmosphere. λ_{ex} = 320 nm, 200 μJcm^{-2}.

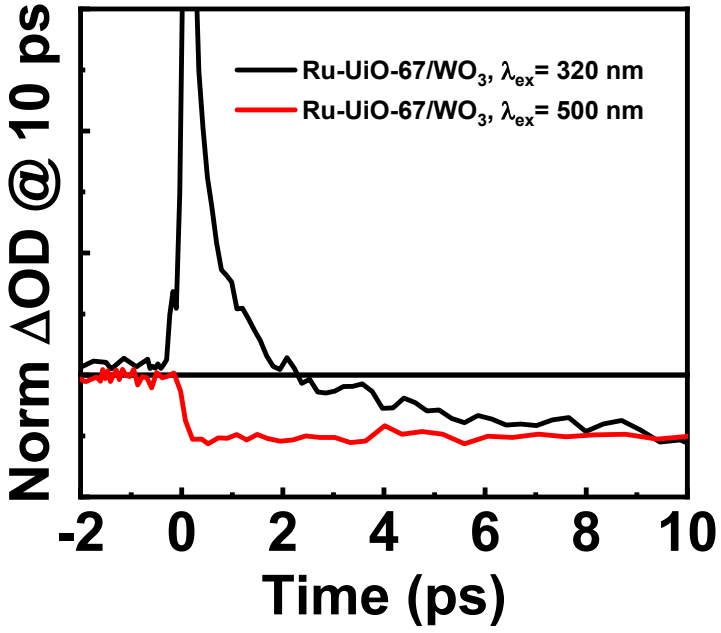

Figure S10. Ultrafast transient absorption kinetics of Ru-UiO-67/WO_3 at the ground-state bleach minima with 500 nm excitation (direct ^{1}MLCT transition, red trace) and 320 nm excitation (higher-energy transitions, black trace). With the 500 nm excitation wavelength there is no short-lived positive absorption feature that 320 nm excitation provides, which supports the notion that higher energy excitations yield short-lived intermediates in the $[Ru(tpy)(dcbpy)OH_2]^{2+}$ catalyst. E_{320nm} = 200 μJ/cm^{-2}, E_{500nm} = 320 μJ/cm^{-2}.

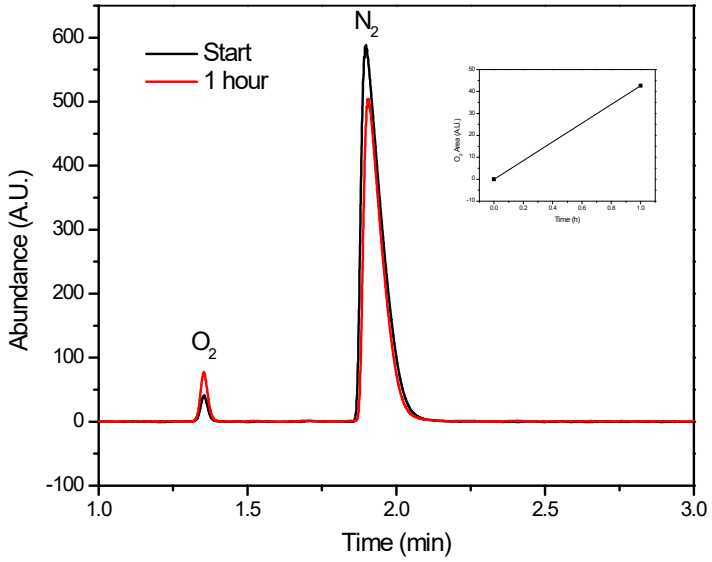

Figure S11. Gas chromatograph of the reaction cell headspace before and after 1 hour of water oxidation catalysis.

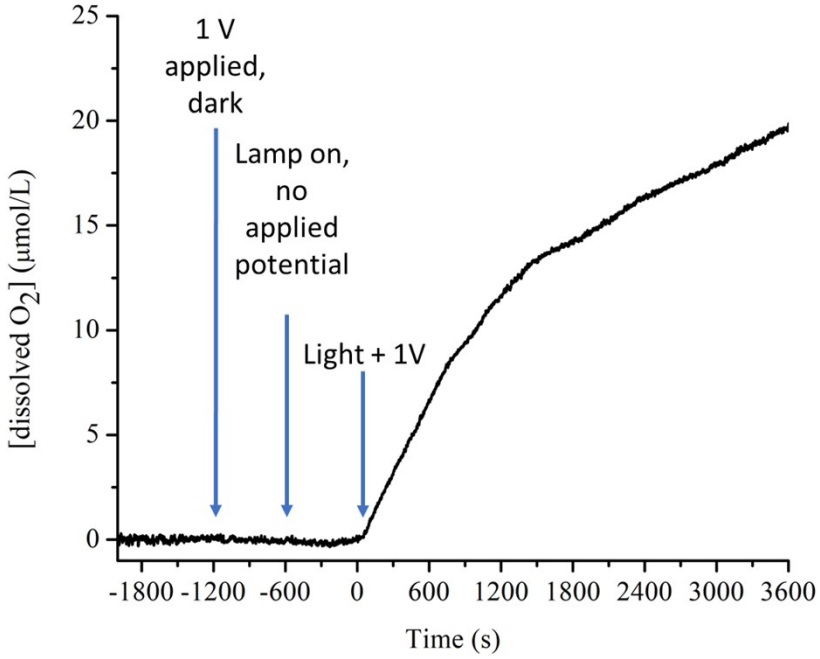

Figure S12. Oxygen production of Ru-UiO-67/WO_3 at 1 V vs. NHE. Catalysis occurs only in the presence of both 1V and photo illumination.

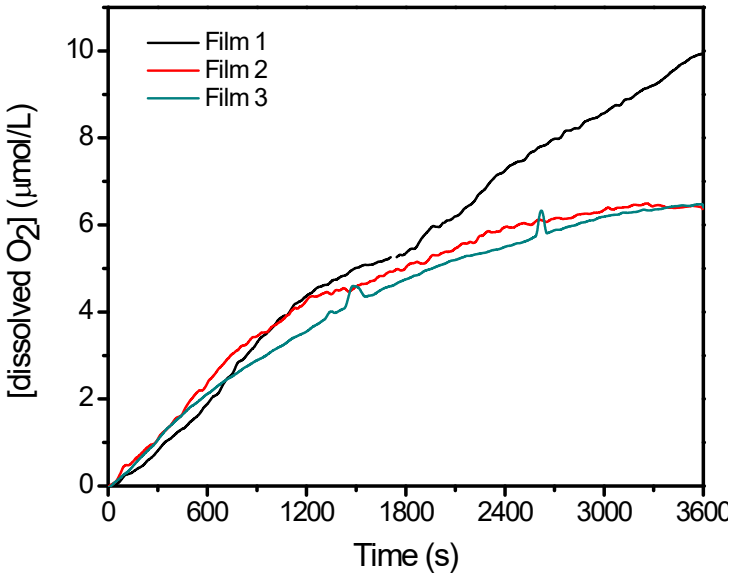

Figure S13. Three Ru-UiO-67/WO_3 films tested for photoelectrochemical water oxidation that were averaged together for activity in the main text.

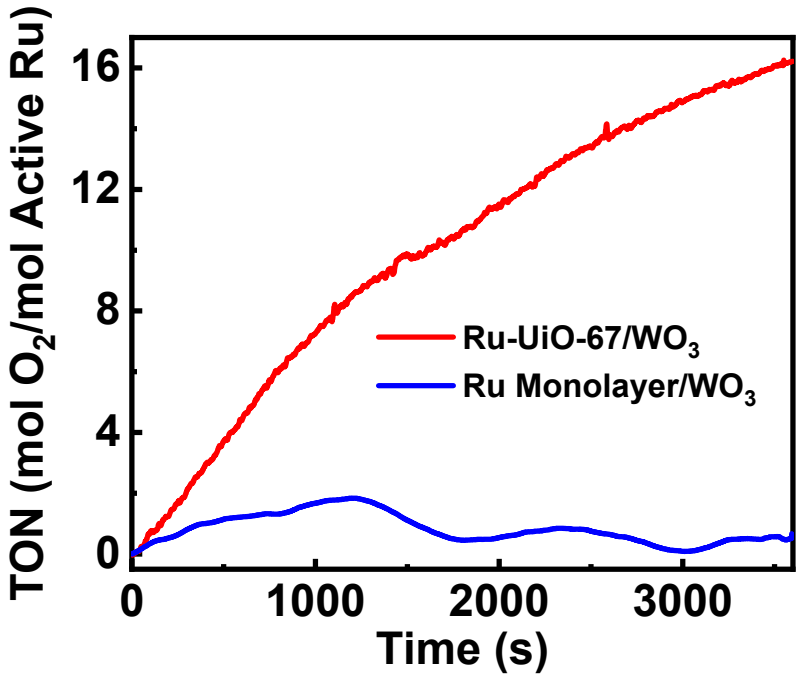

Figure S14. Turnover number (TON) comparison of Ru-UiO-67/WO_3 (red line) to a monolayer of $[Ru(tpy)(dcbpy)OH_2]^{2+}$ on WO_3 (blue line).

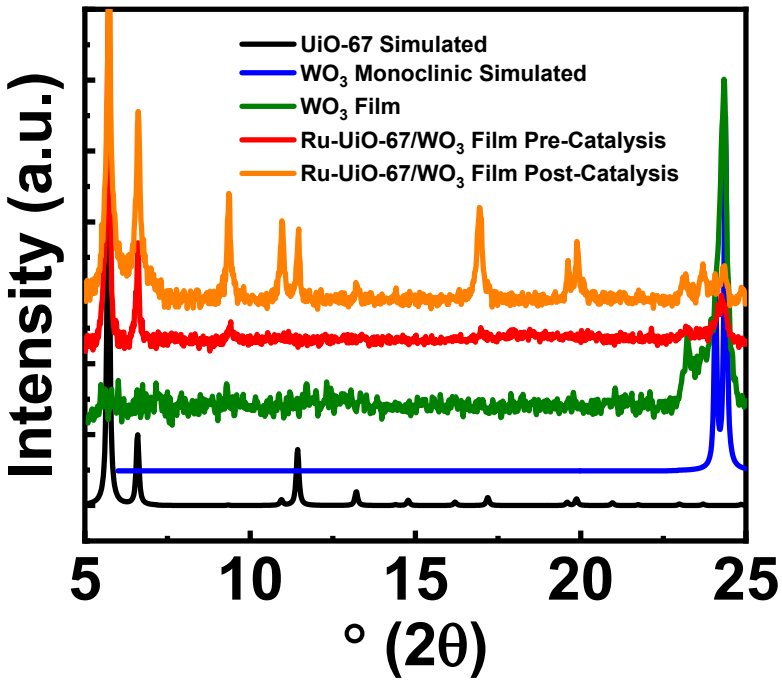

Figure S15. Powder X-ray Diffraction (PXRD) patterns of a Ru-UiO-67/WO_3 film post-catalysis (orange line), Ru-UiO-67/WO_3 film before catalysis (red line), WO_3 film (green line), simulated monoclinic WO_3 pattern (blue) and simulated UiO-67 pattern (black).

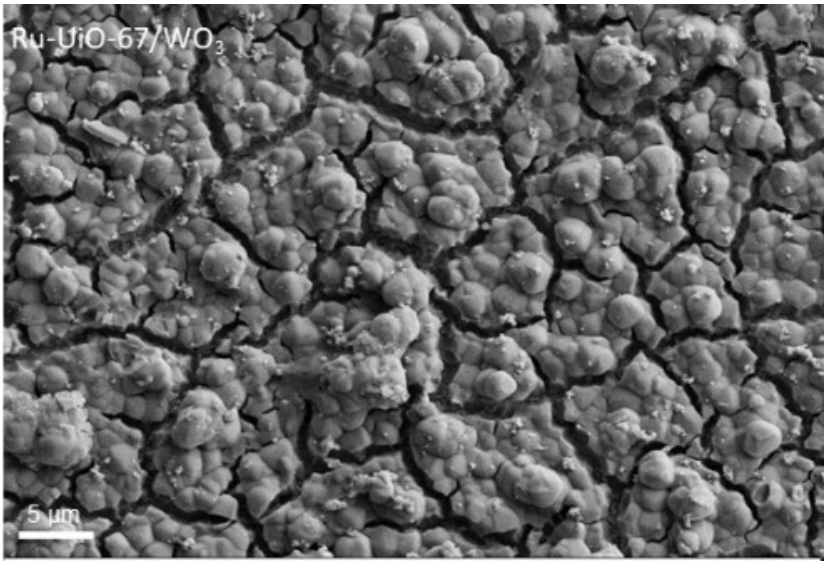

Figure S16. Post-catalysis SEM of Ru-UiO-67/WO_3 showing no significant changes in the morphology of the MOF film.

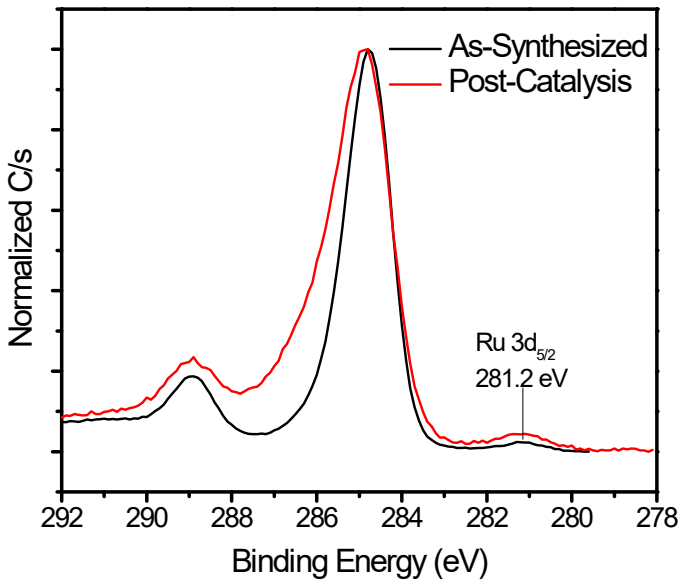

Figure S17. XPS of Ru-UiO-67/WO_3 as-synthesized and post catalysis with no shift observed in the Ru $3d_{5/2}$ region, suggesting the film is stable and does not degrade to RuO_2.

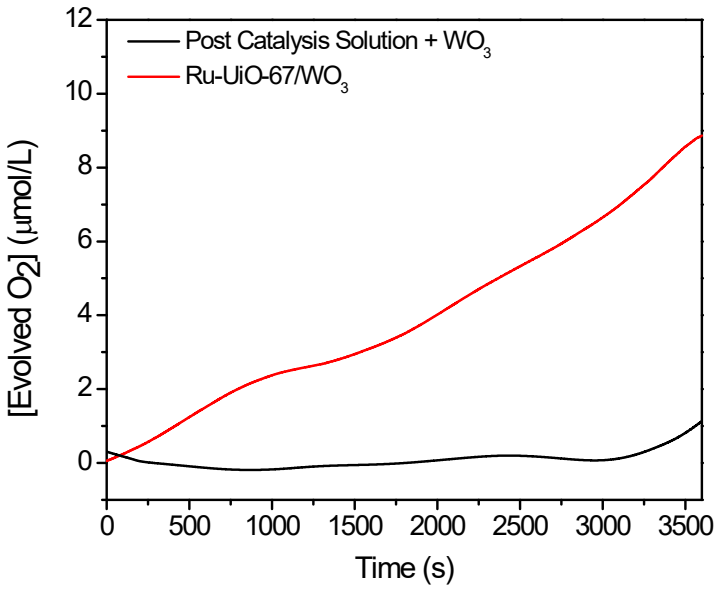

Figure S18. O_2 production of Ru-UiO-67/WO_3 compared to the post-reaction solution with a blank WO_3 electrode.

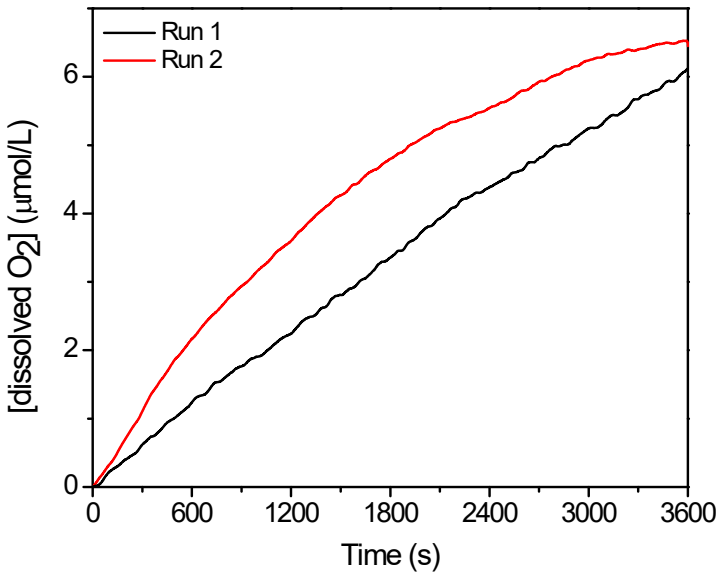

Figure S19. Ru-UiO-67/WO_3 film reused for a second time with no loss of catalytic activity.